Journal of Applied Polymer Science

Cardanol grafted natural rubber: A green substitute to natural rubber for enhancing silica filler dispersion

Sunita Mohapatra,[1] Rosamma Alex,[2] Golok Bihari Nando[1]
[1]Rubber Technology Centre, Indian Institute of Technology Kharagpur, Kharagpur, West Bengal 721302, India
[2]Rubber Research Institute of India, Rubber Board, Kottayam, Kerala 686009, India
Correspondence to: G. B. Nando (E-mail: golokb@rtc.iitkgp.ernet.in)

ABSTRACT: Natural rubber (NR) usage is wide-spread from pencil erasers to aero tyres. Carbon black and silica are the most common reinforcing fillers in the rubber industries. Carbon black enhances the mechanical properties, while silica reduces the rolling resistance and enhances the wet grip characteristics. However, the dispersion of polar silica fillers in the nonpolar hydrocarbon rubbers like natural rubber is a serious issue to be resolved. In recent years, cardanol, an agricultural by-product of the cashew industry is already established as a multifunctional additive in the rubber. The present study focuses on dispersion of silica filler in natural rubber grafted with cardanol (CGNR) and determination of its technical properties. The optimum cure time reduces and the cure rate increases for the CGNR vulcanizates as compared to that of the NR vulcanizates at all loadings of silica varying from 30 to 60 phr. The interaction between the phenolic moiety of cardanol and the siloxane as well as silanol functional groups present on the silica surface enhances the rubber–filler interaction which leads to better reinforcement. The crosslink density and bound rubber content are found to be higher for the silica reinforced CGNR vulcanizates. The physico-mechanical properties of the silica reinforced CGNR vulcanizates are superior to those of the NR vulcanizates. The CGNR vulcanizates show lower compression set and lower abrasion loss. The dynamic-mechanical properties exhibit less Payne effect for silica reinforced CGNR vulcanizates as compared to the NR vulcanizates. The transmission electron photomicrographs show uniform dispersion of silica filler in the CGNR matrix. © 2015 Wiley Periodicals, Inc. J. Appl. Polym. Sci. **2016**, *133*, 43057.

KEYWORDS: biomaterials; elastomers; grafting; morphology; rubber

Received 16 May 2015; accepted 16 October 2015
DOI: 10.1002/app.43057

INTRODUCTION

Natural rubber (NR) consumption across the world is around 43% of the total rubber consumption[1] and in India, it accounts for around 67% of the total rubber consumed as per the recent statistical analysis by the International Rubber Study Group. As per the reports by Indian Rubber Statistics,[2] for the year 2012–2013, the tyre sector consumes around 65% of the total NR produced while 35% is consumed by the non-tyre sector as shown in Figure 1.

The successful use of the rubber products made from natural rubber requires reinforcement by the carbon black and other non-black fillers. In the rubber industry, silica is the most commonly used non-black reinforcing filler because it possesses certain advantages over that of carbon black such as higher tear strength, better abrasion resistance and lower rolling resistance. The silica filler being white is often used in producing white as well as coloured articles.[3] For the same reason, replacement of carbon black by silica has been growing steadily, especially in the tire industry, since the introduction of the "Green Tire Technology" by Michelin in 1992.[4]

Two main factors that contribute to the use of silica fillers in rubber for reinforcement are the filler dispersion and the filler to rubber interaction.[5,6] As per the study, the silica surface is densely populated with siloxane and silanol groups (four to five SiOH groups per 100 $Å^2$)[7] which makes the silica filler polar. The hydrocarbon rubbers like natural rubber, styrene- butadiene rubber and butadiene rubber are nonpolar. Thus, the conventional silica is not compatible with these hydrocarbon rubbers and the problem arises as the filler particles are highly aggregated due to greater filler-to-filler interactions, resulting in a lower dispersion within the rubber matrix and poor mechanical properties. Although silane coupling agents can enhance interaction between silica and the rubber, they only serve a minor effect on improving the dispersion of fillers in rubber.[6] Moreover, the highly dispersible silica technology, as it is used now-a-days, employs mainly solution-polymerized synthetic rubbers and is still not fully commercially feasible with natural rubber.[8]

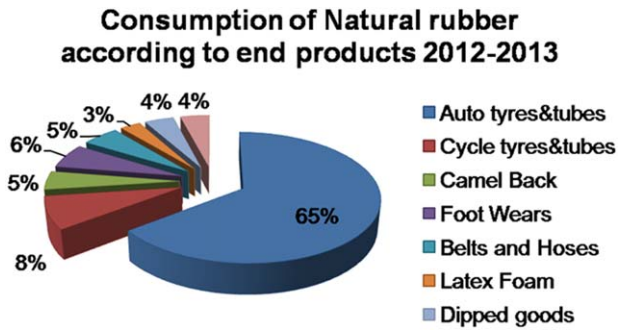

Figure 1. Consumption of natural rubber in India according to end products estimated for the year 2012–2013. [Color figure can be viewed in the online issue, which is available at wileyonlinelibrary.com.]

In the recent years, as silica filler has become an active, high-performance additive for rubber, dispersion of silica particles is of utmost importance to improve reinforcement in the rubber matrices.[9] Therefore, improving the dispersion of silica in rubber and enhancing interaction between silica surface and rubber matrix have thrown open challenges in the arena of rubber research.

Introducing certain functional groups in to the natural rubber backbone would enhance its capability of interaction with the functional groups on the silica surface leading to better rubber-filler interaction and that would facilitate enhanced dispersion of the silica filler. In our earlier work, we have successfully grafted cardanol on to natural rubber in the latex stage at ambient temperature.[10] This has made a great impact in the rubber industry and many industries have shown interest in using it. This is an eco-friendly and techno-economically feasible process.

Cardanol, chemically known as *m*-pentadecenyl phenol, obtained by double vacuum distillation of cashew nut shell liquid is an agricultural renewable resource and a by-product of the cashew industry. In the last few decades, cardanol has been found to be a very useful green substitute to many commercial phenolic compounds, because of its bifunctionality, high reactivity, sustainability, low cost, abundancy, and biodegradability.[11–16]

The phenolic moiety of cardanol along with the aliphatic side chain of 15 carbon atoms in the *meta* position to the hydroxyl group, renders it amenable to a variety of chemical reactions. Moreover, the long aliphatic side chain may be a saturated hydrocarbon, a monoene, diene or triene (non-conjugated) as shown in Figure 2. Cardanol and its derivatives have wide range of applications in the form of brake linings, surface coatings, paints, and varnishes because of its bifunctional moiety and high chemical reactivity. Recently it has been used in the polymer and rubber industries as a multifunctional additive.[17–24]

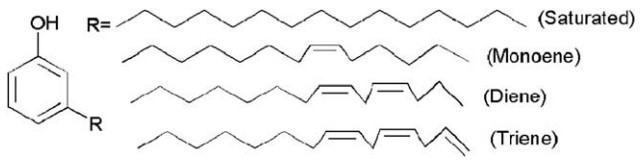

Figure 2. Structure of cardanol.

Table I. Formulation for Preparation of the Silica-filled Rubber Vulcanizates

	Amount, Phr	
Ingredient	NR-S-X	CGNR-S-X
NR	100	-
CGNR	-	100
ZnO	5	5
Stearic acid	2	2
6-PPD	1	1
Precipitated silica (VN3)	0,30,40,50,60	0,30,40,50,60
Si69	0,3,4,5,6	0,3,4,5,6
PEG	0,0.6,0.8,1,1.2	0,0.6,0.8,1,1.2
CBS	0.6	0.6
Sulfur	2.5	2.5

The focus of this article is to utilize the bifunctionality of cardanol to improve the rubber–filler interaction making use of the phenolic moiety as *in situ* reinforcement enhancer. The effect of the grafted cardanol on the physico-mechanical and dynamic mechanical properties of precipitated silica (VN3 grade) filled natural rubber is evaluated.

EXPERIMENTAL

Materials

Natural rubber latex (60.02% DRC) was supplied in kind by Rubber Board, Kottayam, India. Cardanol was procured from M/S Satya Cashew Chemicals Limited, Chennai, India. Zinc oxide, stearic acid, *N*-(1,3-dimethylbutyl)-*N*'-phenyl-*P*-phenylenediamine (6-PPD), *N*-cyclohexyl-benzenesulfonamide (CBS) and sulfur were of the commercially available rubber grades. The filler precipitated silica (VN3 grade) was of laboratory grade. Si69 (Bis[3-(triethoxysilyl) propyl] tetrasulfide, TESPT) employed as the coupling agent was procured from Degussa, Germany. Polyethylene glycol (PEG) was procured from E-Merck, India.

Preparation of the Rubber Vulcanizates

The cardanol-grafted natural rubber (CGNR) was prepared at ambient temperature as described in the earlier publication. The percent grafting was 8.25% and the grafting efficiency was 82.5%.[10] The formulation used for preparation of the rubber vulcanizates is given in Table I. The rubber compounding was carried out on a two-roll mixing mill (Length × Diameter = 330 mm × 152 mm) as described in ASTM D-3182-07 at a friction ratio of 1:1.2. The cure characteristics of the rubber compounds were determined at 150°C by a Rubber Process Analyzer at a strain of 0.5° arc and 100 cpm frequency as per ASTM D-5289-07. Then, the rubber compounds were compression molded into sheets of ~2-mm thick at 150°C using hydraulic hot press (model David Bridge) according to their respective optimum cure times. In sample designation, X refers to the amount of filler in phr incorporated in to the rubber.

Characterization Techniques

Physico-Mechanical Properties. Tensile properties are measured in a Hounsfield tensile testing machine (model H10KS), at a cross head speed of 500 mm min^{-1} as per ASTM D-412-06 (method A). Tear strength of the specimens are determined as per ASTM D-624-00 (Type C die was used to prepare the test specimens). Hardness is measured as per ASTM D-2240-05, using an indentation hardness tester (Type shore A). Compression set at constant strain is carried out according to ASTM D-395-03 (method B). The abrasion resistance is determined by a DuPont abrader as per ISO 4649:2010 (method A).

Bound Rubber Content. The measurement of bound rubber content in rubber compounds has been performed extensively and is considered as a typical feature of surface activity. Bound rubber (BdR) is defined as the rubber portion in an uncured compound, which cannot be extracted by a good solvent because of the adsorption of rubber molecules onto the filler surface.[25] It is determined by extracting the unbound materials such as the compounding ingredients and free rubber in toluene for 3 days followed by drying for 2 days at room temperature. The weight of the samples before and after the solvent extraction is measured, and the bound rubber content is calculated using eq. (1).

$$\mathrm{BdR}=\frac{W\mathrm{fg}-Wt\left(\frac{mf}{mf+mr}\right)}{Wt\left(\frac{mf}{mf+mr}\right)}\times 100 \tag{1}$$

where W_{fg} is the weight of filler and gel, W_t is the weight of the sample, m_f is the fraction of the filler in the compound and m_r is the fraction of the rubber in the compound.

Swelling Study. Circular test pieces with a radius of 20 mm are cut from a molded sheet having a thickness of 1.5–2.0 mm. The accurately weighed samples are immersed in toluene at room temperature up to equilibrium swelling, and the swollen samples are weighed accurately. The volume swelling[26] is calculated using eq. (2).

$$\%\ \text{swelling by volume}=\left({}^{W_2}/_{W_1}-1\right){}^{\rho_r}/_{\rho_s}\times 100 \tag{2}$$

Where, W_1 and W_2 are the weights of the specimens before and after swelling, respectively and ρ_r and ρ_s are the densities of the specimen and the test solvent, respectively.

The crosslink density is measured by equilibrium swelling method using toluene as solvent. Flory–Rehner equation[27] is employed to calculate crosslink density as given in eq. (3).

$$-\ln(1-v_r)-v_r-\chi v_r{}^2=2v_s\eta(v_r{}^{1/3}-2v_r/f) \tag{3}$$

where v_r is the volume fraction of the rubber in the swollen sample, v_s is the molar volume of solvent (106.2 g mol^{-1} for toluene), χ is the Flory–Huggins polymer–solvent interaction parameter (value of χ is 0.36 at 30°C). η is the crosslink density of rubber (mol cm^{-3}) and f is functionality of the crosslinks (being 4 for sulfur curing system).

The volume fraction of rubber, v_r is calculated by the expression given by Ellis and Welding[28]:

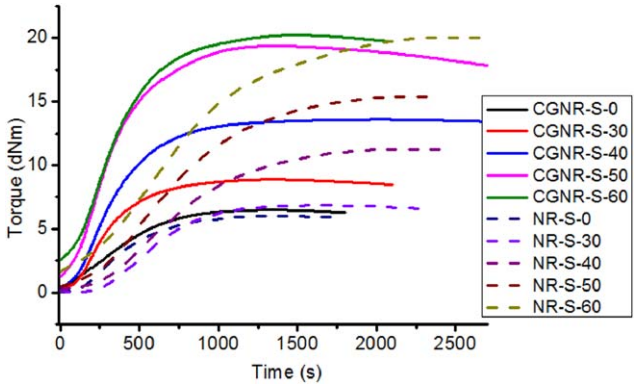

Figure 3. Rheographs of gum and silica-filled NR and CGNR vulcanizates. [Color figure can be viewed in the online issue, which is available at wileyonlinelibrary.com.]

$$v_r=\frac{(D-FT)\rho_r{}^{-1}}{(D-FT)\rho_r{}^{-1}+(A_0\rho_s{}^{-1})} \tag{4}$$

where, T is the weight of the test specimen, F is the weight fraction of the insoluble components in the sample, D is the deswollen weight of the test specimen, A_0 is the weight of absorbed solvent, ρ_r is the density of the rubber and ρ_s is the density of solvent (0.87 g cm^{-3} for toluene).

Field Emission Scanning Electron Microscopy. The morphology of the tensile and abrasive fracture surface of the NR and CGNR vulcanizates are studied in a field emission scanning electron microscope (model Supra40, Carl Zeiss SMT AG, Oberkochen, Germany). The samples are mounted on aluminum (Al) stubs and its surfaces are gold (Au) coated by means of manually operated sputter coater (model SC7620, Polaron Brand, Quorum Technologies, East Sussex, UK) machine.

High Resolution Transmission Electron Microscopy. The dispersion of the fillers was studied by high resolution transmission electron microscope (Model-JEM-2100 HRTEM, JEOL Limited, Tokyo, Japan, Point to point resolution—0.194 nm, Lattice resolution—0.14 nm, Tilt Angle: 24°, Acc. Voltage: 200 kV, Filament: LaB6). The HRTEM images of the samples were captured by means of charge couple device (CCD) multiscan camera (model 794, Gatan, CA) using the Gatan Digital Micrograph 3.1 software package. The samples were prepared using an ultramicrotome (Ultracut R, Leica) equipped with a diamond knife and then supported on copper grids before observation under the microscope.

Dynamic Mechanical Analysis. Dynamic mechanical properties of the vulcanizates were determined with the help of a Dynamic Mechanical Analyzer (Metravib DMA).The measurements were done under tension mode in the temperature range from −80°C to +100°C at a heating rate of 2°C min^{-1} with 0.1% strain and 1 Hz frequency. The strain sweep measurements were performed at ambient temperature at a frequency of 10 Hz.

RESULTS AND DISCUSSION

Cure Characteristics

The rheographs of the gum and the silica-filled NR and CGNR compounds with filler loadings varying from 30, 40, 50, to 60 phr are shown in Figure 3 and the cure chacteristics are presented in Table II.

Table II. Cure Characteristics of the Silica-filled NR and CGNR Vulcanizates

Sample code	Minimum torque (dNm)	Maximum torque (dNm)	Delta torque (dNm)	Scorch time, t_2 (min)	Optimum cure time, t_{90} (min)	Cure rate index (min^{-1})
CGNR-S-0	0.11	6.51	6.4	3.00	8.10	19.61
CGNR-S-30	0.18	8.89	8.71	2.95	11.30	11.98
CGNR-S-40	0.37	13.71	13.34	2.75	13.00	9.76
CGNR-S-50	1.28	19.68	18.4	2.25	13.08	9.23
CGNR-S-60	2.62	20.59	17.97	2.12	13.20	9.02
NR-S-0	0.06	6.03	5.97	4.87	12.92	12.42
NR-S-30	0.09	7.02	6.93	7.40	16.58	10.89
NR-S-40	0.23	11.4	11.17	6.95	22.12	6.59
NR-S-50	0.48	15.68	15.2	5.43	22.47	5.87
NR-S-60	1.67	20.34	18.67	4.40	23.60	5.21

It is observed that for both NR and CGNR compounds, the optimum cure time increases with increase in the silica filler loadings; however, the scorch time decreases. The cure rate index which is a measure of the cure rate of the rubber is found to be decreased with increase in the filler loading for both the rubber compounds i.e., from 12.42 to 5.21 min^{-1} for NR compounds and 19.61–9.02 min^{-1} for the CGNR compounds. The surface of silica fillers possess siloxane and silanol groups which make these fillers acidic. They interact with basic accelerators resulting in detrimental effects on the cure characteristics such as retarding the cure rate and increasing the optimum cure time.[29] However, it can be seen that, the cure rate is higher for the CGNR compound in comparison with that of NR compound having similar filler loadings. This may be interpreted as due to the participation of the unsaturation present in the side chain of cardanol in the curing reaction.[30,31] Moreover, the optimum cure time and the scorch time for the CGNR compound is lower than that of the NR compound. Delta torque is defined as the difference between the maximum and minimum torques. Because the torque in the rheograph starts to increase with the formation of crosslinks within the rubber compounds, delta torque is very closely related to the crosslink density; the larger the delta torque, the higher will be the crosslink density.[32–34] From Table II, it can be seen that the delta torque for the CGNR compound is higher than that of the NR compound at the same loadings of silica filler exception to 60 phr. The higher delta torque infers a higher crosslink density for the CGNR vulcanizate in comparison with that of the NR vulcanizate.

Bound Rubber Content and Crosslink Density

Rubber-to-filler interaction plays a major role in enhancing properties of rubber vulcanizates. The measurement of bound rubber is a practical means of evaluating the degree of rubber-filler interaction. Bound rubber may be defined as the rubber material that cannot be separated from the filler when the uncured rubber compound is extracted in a solvent in which the rubber is readily soluble.[29] The bound rubber content is a quantitative measurement of the filler surface activity and the rubber–filler interactions.

Figure 4(a) shows the variation of the bound rubber content of the NR and CGNR compounds at silica filler loadings varying from 30 to 60 phr. It is seen that the bound rubber content increases with increase in filler loadings for both NR and CGNR compounds. However, the bound rubber content is higher for silica-filled CGNR compound as compared to that of NR compound at similar filler loadings. Wolf *et al.*[25] have

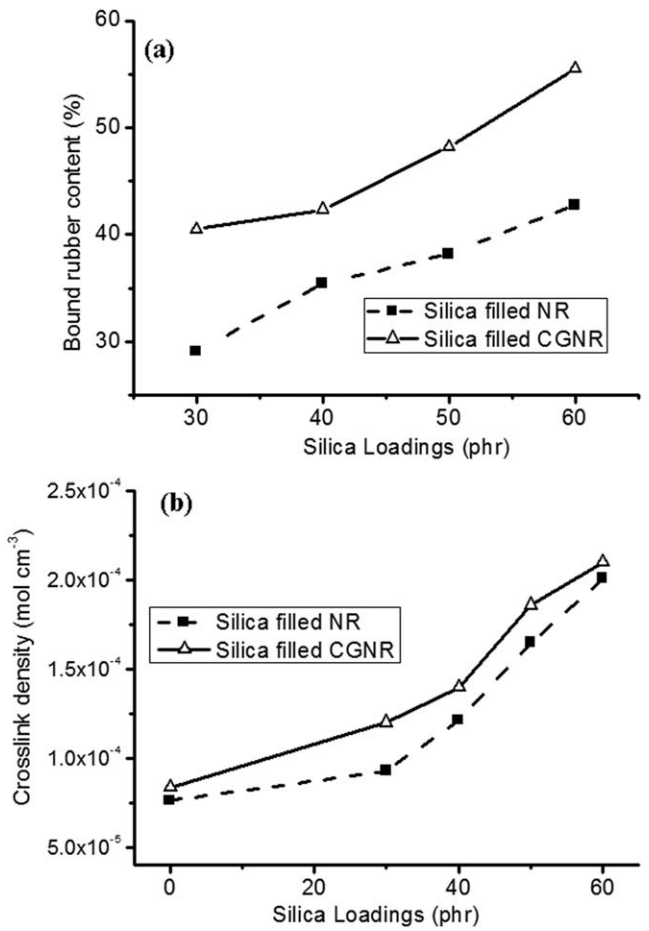

Figure 4. Crosslink density (a) and bound rubber content (b) of the silica-filled NR and CGNR vulcanizates.

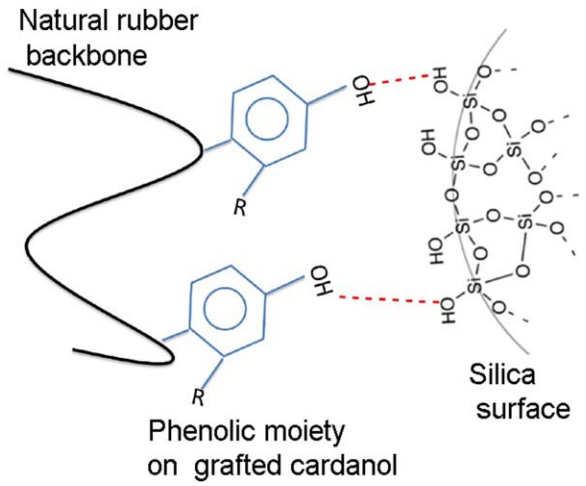

Figure 5. Schematic presentation of interaction of silica surface with cardanol moiety present in CGNR. [Color figure can be viewed in the online issue, which is available at wileyonlinelibrary.com.]

concluded that the filler–polymer interaction leads to the formation of bound rubber that involves physical adsorption, chemical adsorption, and physical interaction amongst which chemical adsorption plays a very significant role. It is the reactive sites in both the elastomer and the filler surface which are primarily responsible for bound rubber formation.[35] The higher bound rubber content in the CGNR compounds may be attributed to the formation of hydrogen bonds between the functional groups like siloxane and silanol groups present on the silica surface with the phenolic —OH group present in the cardanol moiety of the grafted natural rubber which has been schematically presented in Figure 5.

The crosslink density of the gum and silica filled NR as well as CGNR vulcanizates are shown in Figure 4(b). It is observed from the Figure 4(b) that the crosslink density increases with increase in the silica filler loading for both NR and CGNR vulcanizates. However, the crosslink density for the CGNR vulcanizates is higher than that of the NR vulcanizates at each loading of the silica filler which supports the results obtained from the cure characteristics. The participation of the unsaturation present in the aliphatic side chain of cardanol in the vulcanization reaction of the rubber is responsible for the higher crosslink density of the CGNR vulcanizates.[30]

Rubber–Filler Interaction and Reinforcement Phenomenon

Swelling Study. The swelling behavior of the vulcanizates bears a close relation with the rubber–filler interactions and crosslink density of the filled vulcanizates. Figure 6 represents the dependency of the percent swelling against silica loading for the NR and CGNR vulcanizates. It can be seen that, the gum vulcanizates impart higher swelling percentage than the silica filled vulcanizates irrespective of the rubber matrices. The gum vulcanizates show a volume swelling of 410% for NR and 364% for CGNR vulcanizate. However, the percent volume swelling of the rubber gradually decreases with increase in the filler loading as expected due to the reinforcing effect of the silica filler in the rubber matrix. This is also evident from the reduction in the percentage of swelling of the vulcanizates with increase in the filler loading. A sharp fall in the volume swelling is observed up to 40 phr silica filler loading; i.e. the volume swelling reduces to 237% for 40 phr silica filled NR vulcanizates while, it reduces to 206% for 40 phr silica-filled CGNR vulcanizates. Afterward, it gradually drops down to 158% for 60 phr silica-filled NR vulcanizates and 147% for 60 phr silica-filled CGNR vulcanizates. Moreover, it is observed in general that, the percent swelling is much lower for the CGNR vulcanizates than that of the NR vulcanizates at each loading of the silica filler. This may be attributed to the higher rubber–filler interaction, exhibited by the CGNR matrix due to the greater interaction between the phenolic moiety of cardanol and the surface functional groups present on the silica as shown schematically in Figure 5.

The extent of rubber–filler interaction may be evaluated by using Cunneen and Russell equation as presented in eq. (5).

$$\frac{V_{ro}}{V_{rf}} = ae^{-z} + b \tag{5}$$

where V_{ro} and V_{rf} are the volume fractions of rubber in the swollen gel for the gum and filled rubber vulcanizates, respectively in presence of the solvent toluene, z is the weight fraction of the filler in the vulcanizate and, "a" and "b" are constants. A plot of V_{ro}/V_{rf} against e^{-z} is linear with the slope "a" and intercept "b." The higher the value of "a" and the lower value of "b" indicate higher swelling restriction and better rubber–filler interaction.[36] Figure 7(a) shows the Cunnen–Russel plot for the silica filled NR and CGNR vulcanizates. It can be seen from Figure 7(a) that the slope, "a" is higher for CGNR vulcanizates ($a = 5.65$) in comparison with that of NR vulcanizates ($a = 4.67$) and the intercept, "b" is found to be lower for CGNR vulcanizates ($b = -4.66$), while that for NR vulcanizates, the value is $b = -3.66$. This indicates that the rubber–filler interaction is more in case of silica filled CGNR vulcanizates in comparison with that of NR vulcanizates.

Another model is also applied for the quantitative measurement of the rubber–filler interaction and reinforcement of fillers in the rubbers popularly known as Kraus model.[37] This has been expressed as:

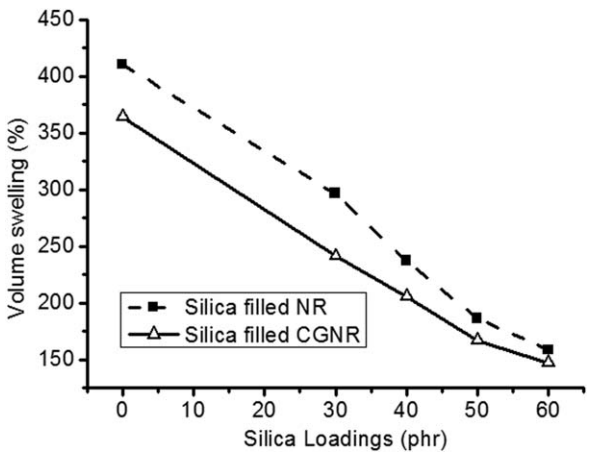

Figure 6. Volume swelling of NR and CGNR vulcanizates in toluene as solvent.

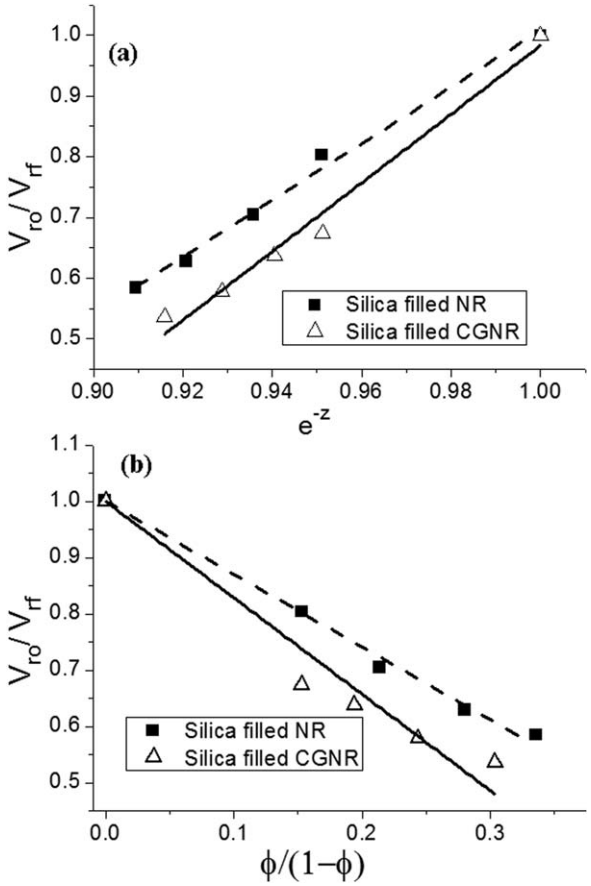

Figure 7. (a) Cunneen–Russell Plot and (b) Kraus plot for silica-filled NR and CGNR vulcanizates.

$$\frac{V_{ro}}{V_{rf}} = 1 - m\left(\frac{\phi}{1-\phi}\right) \quad (6)$$

where φ is the volume fraction of filler in the filled vulcanizates, and "m" is the slope of linear fit in the Kraus model. A plot of V_{ro}/V_{rf} against $\varphi/(1-\varphi)$ is linear and exhibits a negative slope, indicative of the reinforcement phenomenon. The higher the negative slope, greater is the reinforcement. The slope "m" gives the degree of interaction between the rubber and the filler.

The ratio V_{ro}/V_{rf}, represents the degree of restriction of the swelling of rubber matrix because of the presence of filler as compared to that without filler. The Kraus plots for the NR and CGNR vulcanizates are shown in Figure 7(b). According to Kraus[37] if the filler swells just as much as the rubber matrix, the vulcanizates will be uniform and the value of V_{ro}/V_{rf} will be equal to the gum. However, most fillers are not soluble in the organic solvents, hence, will not be swollen in the solvent. Thus, the rubber molecules attached to the filler surface shall restrict the movements of the matrix, and the solvent will not be able to penetrate the interstices of the rubber chains. This result in lower swelling of the matrix compared to the gum vulcanizates, leading to a decrease in the V_{ro}/V_{rf} ratio with increase in the filler loading. On the other hand, if the filler imparts no effect on the matrix, the ratio shall increase with increasing the amount of filler.[38] Thus, in case of gum vulcanizate, the ratio of V_{ro}/V_{rf} shall be unity, which may be referred as the standard swelling ratio. If $V_{ro}/V_{rf} > 1$, the filler and the rubber have no interaction and show an increase with filler loading. On the other hand, if the ratio $V_{ro}/V_{rf} < 1$, there is interaction between the filler and the rubber and the ratio shall decrease steadily with increase in filler loading. It is seen from Figure 7(b) that the ratio V_{ro}/V_{rf} decreases with increasing the volume fraction of filler and $V_{ro}/V_{rf} < 1$ for both NR and CGNR vulcanizates. However, this decrease is more pronounced in case of CGNR-silica filled vulcanizates. This infers that, the rubber chains are adhered to the filler surface more strongly in the CGNR matrix than NR matrix. The extent of filler reinforcement in the rubber matrix can be calculated from the slope of the linear plot. The greater the interaction between the rubber matrix and the filler, the more will be the swelling resistance caused by the filler and the higher will be the negative value of the slope, "m." The slope for CGNR vulcanizates is found to be -1.71 in comparison with that obtained for NR vulcanizates ($m = -1.24$). This is a clear evidence of greater rubber–filler interaction for the CGNR vulcanizates filled with precipitated silica as compared to that of NR vulcanizates filled with the said silica. This has been attributed to the polar–polar interaction and hydrogen bond formation between the functional groups like siloxane and silanol groups present on the silica surface and the phenolic —OH group present in the cardanol moiety in case of the cardanol grafted natural rubber as discussed.

Payne Effect. Payne effect is defined as the decrease in storage modulus with increase in strain amplitude showing a nonlinear behavior in case of the filled rubbers when there is no or less interaction between the filler and the rubber and more between filler and filler. The storage modulus of gum rubbers does not change significantly with increasing strain amplitude; however it decreases in case of the filled rubber showing a typical nonlinear relationship.[39] Payne effect can be calculated from the difference of the storage modulus as $\Delta G' = G'_0 - G'_\infty$, where G'_0 is the storage modulus at low strain amplitude and G'_∞ is the storage modulus at high strain amplitude.

Payne effect reflects the formation of filler network in the polymer matrix. The rubber trapped or caged in the filler network, loses its identity as an elastomer and behaves as a filler in terms of stress–strain properties.[5] At lower strain, the filler network cannot be broken, and thus, at higher filler loadings more filler networks are formed leading to increase in storage modulus. Whereas, at higher strain amplitude the filler network breaks down and the trapped rubber is released, so that the effective volume fraction of the filler is reduced and hence, decreases the storage modulus. The decrease in storage modulus with increase in strain amplitude has been explained as a consequence of the breakage of physical bonds between the fillers, and more appropriately, the breakage of three-dimensional network of the silica aggregates and agglomerates. When the strain is high enough to destroy the filler networks, the moduli of compounds decrease to almost the same level as that contributed by the rubber matrix.[40]

For a filled rubber compound, the Payne effect reflects the strength of the filler network structure. Lower the storage

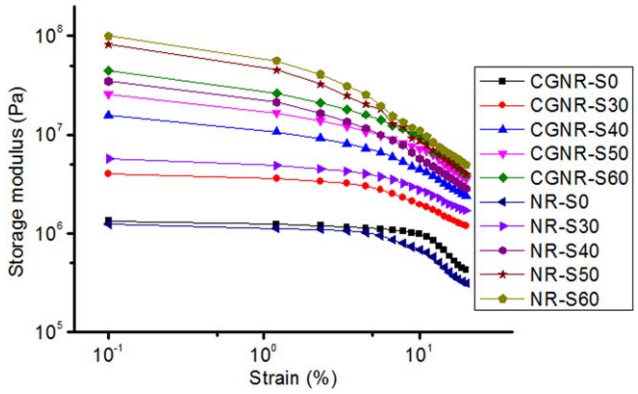

Figure 8. Storage modulus as a function of strain (%) for the gum and silica filled NR and CGNR vulcanizates. [Color figure can be viewed in the online issue, which is available at wileyonlinelibrary.com.]

modulus at small strains, weaker is the filler–filler network structure. From Figure 8, it is observed that with increase in filler loading, the low strain modulus increases for both NR and CGNR vulcanizates which indicates the formation of more filler–filler networks at higher concentration of silica filler loadings. However, the low strain modulus (G'_0) in case of the silica filled CGNR vulcanizates is found to be lower than that observed for the NR vulcanizates at the same loading of the silica filler. This may be because of the fact that, there are less filler–filler networks in the CGNR vulcanizates as compared to that of NR vulcanizates at the same loadings of the filler.

The gum vulcanizate of both the NR and CGNR exhibit no indication of nonlinearity. However, for the filled vulcanizates, the low strain modulus (G'_0) is higher than that of the high strain modulus (G'_∞), resulting in a non-linear viscoelastic behavior giving rise to the Payne effect, which is presented in Table III. From Table III, it is observed that $\Delta G'$ increases with increasing silica filler concentration in both the rubber matrices NR and CGNR; which is an indication of higher Payne effect with increase in silica filler loading. This increase is caused by the formation of filler–filler interactions. This has been attributed to two reasons; (i) increasing silica filler loading results in a decrease in inter-aggregate distances, thus increasing the probability of the formation of a filler network structure and (ii) lack of interaction between the rubber and the filler.[41] Moreover, the silica-filled CGNR vulcanizates show less Payne effect than those of the silica filled NR vulcanizates at the corresponding filler loadings. This may be presumed to be due to higher polymer–filler interaction of the cardanol grafted natural rubber discussed above, causing reduction in the filler–filler interaction. This facilitates better dispersion of the filler in the cardanol grafted natural rubber in comparison with that of the natural rubber.

Table III. G′ Value for Gum and Silica-filled Samples at Low and High Strain and Corresponding ΔG′ Value

	CGNR					NR				
Samples	S-0	S-30	S-40	S-50	S-60	S-0	S-30	S-40	S-50	S-60
G′0 (kPa)	1335	4021	15,673	25,480	43,975	1232	5707	34,462	81,463	99,555
G′∞ (kPa)	426	1182	2401	3566	3906	312	1704	2824	3996	4919
ΔG′ (kPa)	9.1×10^2	2.8×10^3	1.3×10^4	2.2×10^4	4.0×10^4	9.2×10^2	4.0×10^3	3.2×10^4	7.7×10^4	9.5×10^4

Physico-Mechanical Properties

The physico-mechanical properties of the NR and CGNR vulcanizates have been investigated by varying silica filler loadings from 0 to 60 phr and the results are presented in Figure 9. From Figure 9(a) it is seen that the tensile strength increased with silica filler loading up to 40 phr, and then it decreased gradually for both NR and CGNR vulcanizates at higher filler

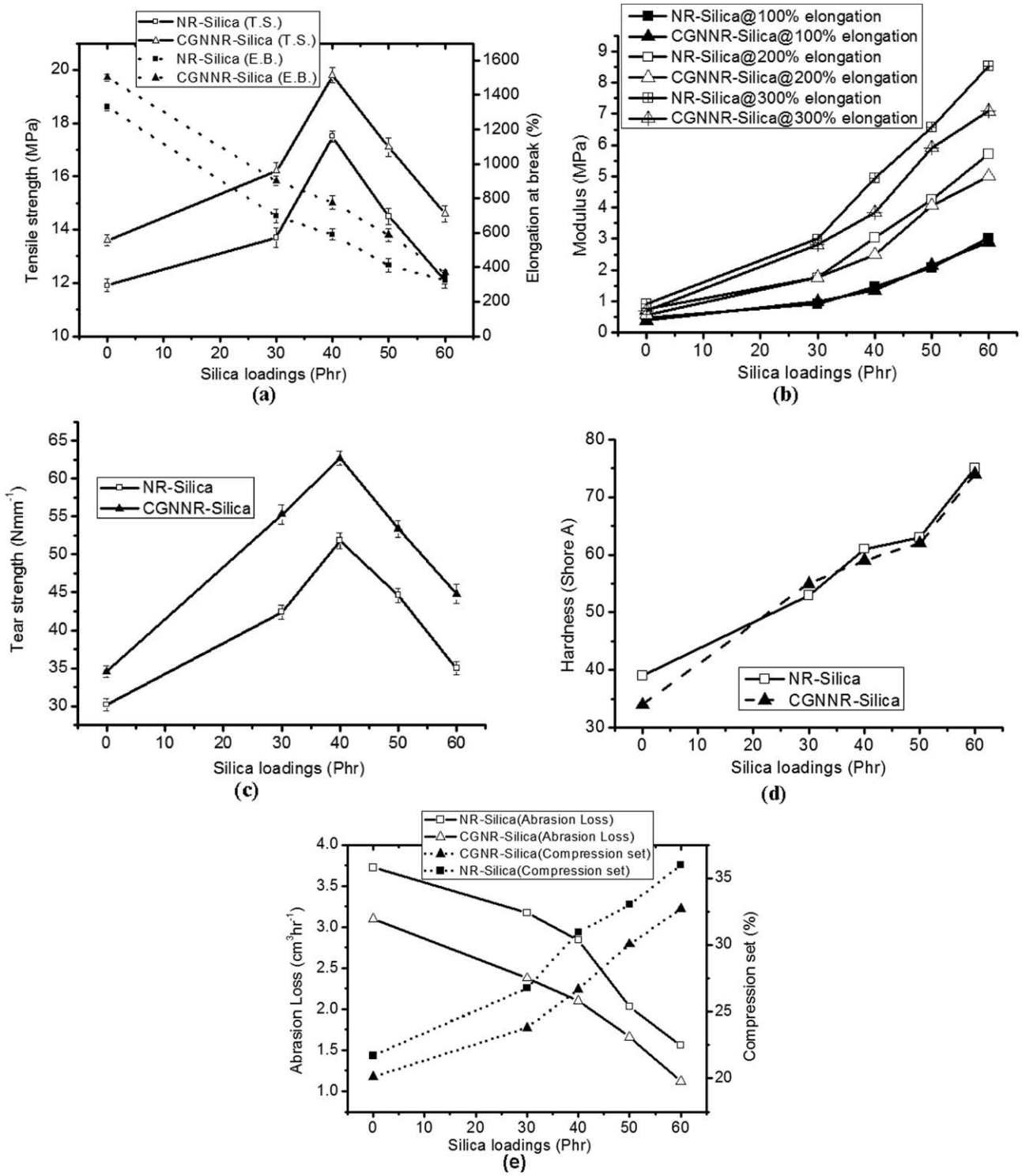

Figure 9. Physico-mechanical properties of silica filled NR and CGNR vulcanizates (a) Tensile strength and Elongation at break (b) Modulus (c) Tear strength (d) Hardness and (e) Abrasion loss and compression set.

loadings. This may be attributed to the dilution effect of the filler and agglomeration tendency of the fine nanoparticles because of higher filler–filler interaction. The tensile strength of gum NR vulcanizates is determined to be 11.9 MPa and it increased up to a value of 17.5 MPa at 40 phr loading of silica filler and then gradually decreased down to 12.1 MPa at 60 phr filler loading. On the other hand, the tensile strength of gum CGNR vulcanizates is found to be 13.6 MPa. It increased up to a value of 19.8 MPa at 40 phr loading of silica filler showing a 13.1% increase over that of NR vulcanizates at equal loading of silica. On further increase in filler content, the tensile strength gradually decreased to 14.6 MPa at 60 phr loading of silica. It is

observed that the tensile strength of CGNR vulcanizates at each level of filler is higher than that of the NR vulcanizate. This has been very well reflected in the Payne effect also which is higher for NR vulcanizates related to that observed for CGNR vulcanizates. The higher tensile strength of the silica filled CGNR vulcanizates may be attributed to the higher crosslink density and higher bound rubber content. Because, silica is hydrophilic and natural rubber is hydrophobic in nature, in silica filled natural rubber compounds, use of a coupling agent establishes very good rubber–filler interaction, hence provides greater reinforcement to the rubber matrix. In addition, in case of CGNR vulcanizates, there is one more type of interaction present between the silica filler and the CGNR matrix, which is the interaction between phenolic —OH group of cardanol and surface —OH group of silica as discussed earlier. The mechanism of interaction has been presented schematically in Figure 5 and this provides greater reinforcement of silica filler in the CGNR matrix.

Figure 9(a) shows the elongation at break of all the vulcanizates with silica filler loading. Elongation at break is found to decrease with increase in silica filler loading in both NR and CGNR vulcanizates. The elongation at break for NR gum vulcanizates is found to be 1329% which reduced gradually to 325% with increase in filler loading up to 60 phr of silica. On the other hand, the elongation at break for the CGNR vulcanizates is higher at every loading of silica. The elongation at break for gum CGNR vulcanizates is 1502% and with increase in filler loading it reduced gradually to 368% with 60 phr loading of silica. This has been attributed to the plasticization effect of the CGNR due to the presence of long aliphatic side chains present in the cardanol, in CGNR vulcanizates.

Modulus is an indication of the relative stiffness of a material. The tensile moduli (100, 200, and 300%) of NR and CGNR vulcanizates increase with increase in the silica filler loading as shown in Figure 9(b). As more and more fillers are incorporated into the rubber matrix, the elasticity of the rubber chains are reduced due to reduction in available free space and restriction in the motion of chains due to interaction with the filler particles resulting in an increase in stiffness. The modulus at 100% elongation is found to be comparable for both the modified and unmodified NR vulcanizates. However, the moduli at 200 and 300% elongation is comparable up to 30 phr loading of silica for both the NR and CGNR vulcanizates and beyond which, the moduli of CGNR vulcanizates are found to be lower than that of the NR vulcanizates at equal loadings of the silica filler.

The tear strength of NR and CGNR vulcanizates [Figure 9(c)] increase with increase in the silica filler loading up to 40 phr beyond which it reduces for both NR and CGNR vulcanizates. The tear strength of gum NR vulcanizate is found to be 30.2 N mm^{-1} which increases up to 51.8 N mm^{-1} for 40 phr loading of the filler, beyond which it decreases to 35.0 N mm^{-1} at 60 phr loading of silica filler. Interestingly, the tear strength of CGNR vulcanizates is found to be invariably higher than that of the NR vulcanizates at equivalent loadings. The tear strength of gum CGNR vulcanizate is found to be 34.6 N mm^{-1} which increases up to 62.7 N mm^{-1} at 40 phr loading of the filler exhibiting an increase by 21% than that of the NR vulcanizate and then decreases to 44.8 N mm^{-1} at 60 phr loading. This has been explained as due to a higher crosslink density and higher bound rubber content of the CGNR vulcanizates supporting the hypothesis explained above.

The hardness of the silica filled NR and CGNR vulcanizates increase with increase in silica loading as shown in Figure 9(d). Because hardness is dependent upon the modulus, it may be interpreted that incorporation of reinforcing filler into the rubber matrix increases the modulus so as the hardness, leading to more rigid rubber composites. The hardness of the gum NR vulcanizate is 39 shore A and increases gradually up to 75 shore A with 60 phr silica filler loading as shown in Figure 9(d). However, the hardness is found to be 34 shore A for the gum CGNR vulcanizate, which increases steadily up to 74 shore A at 60 phr loading of silica filler. The hardness of both the rubber matrices (NR and CGNR) is found to be comparable at all loadings of the silica filler.

One of the major advantages of incorporation of silica filler into the rubber compound is to reduce the abrasion loss and to increase the abrasion resistance to a greater extent. Figure 9(e) shows that, the abrasion resistance increases with an increase in the silica filler loading for both NR and CGNR vulcanizates. The abrasion loss for gum NR vulcanizate is found to be 3.72 $cm^3\ h^{-1}$ which decreases to 1.56 $cm^3\ h^{-1}$ at 60 phr of silica loadings. However, the abrasion loss for gum CGNR vulcanizate which is found to be 3.1 $cm^3\ h^{-1}$ and it decreases to 1.12 $cm^3\ h^{-1}$ at 60 phr silica loading. It has been observed from Figure 9(e) that, the abrasion loss is lower for CGNR vulcanizates in comparison with that of NR vulcanizates at equivalent loading of silica filler. This significant improvement in abrasion resistance may be explained as due to higher rubber–filler interaction, more bound rubber formation and additional crosslink formation for the cardanol grafted natural rubber.

Compression set under constant strain increases with increase in the filler loading for both NR and CGNR vulcanizates as shown in Figure 9(e). This has been explained as due to the decrease in the mobility of the rubber chains in presence of silica fillers because of formation of pseudo crosslinks through fillers resulting in increased stiffness of the vulcanizates. The rubbers are generally incompressible. When the rubber vulcanizate is subjected to compression under high stress or higher strain, definite deformation occurs. If kept for a definite length of time at a relatively higher temperature than the ambient, viscous flow occurs and permanent deformation is observed even after the load is removed. This set is a measure of the stiffness of the rubber composites.[42] Of course, during this process some crosslinks are broken to relieve the stress. The number of crosslinks responsible for the strain recovery is less than the number of crosslinks responsible to resist compression i.e., the initial crosslink density of the rubber. As a result, an increase in silica filler loading in the vulcanizates results in a stiffer matrix. In consequence, there is less probability of flow in the matrix under compressive load. On the other hand, under higher silica filler content in the rubber, the compression set is higher due to higher deformation of the chains and breakage of filler–rubber

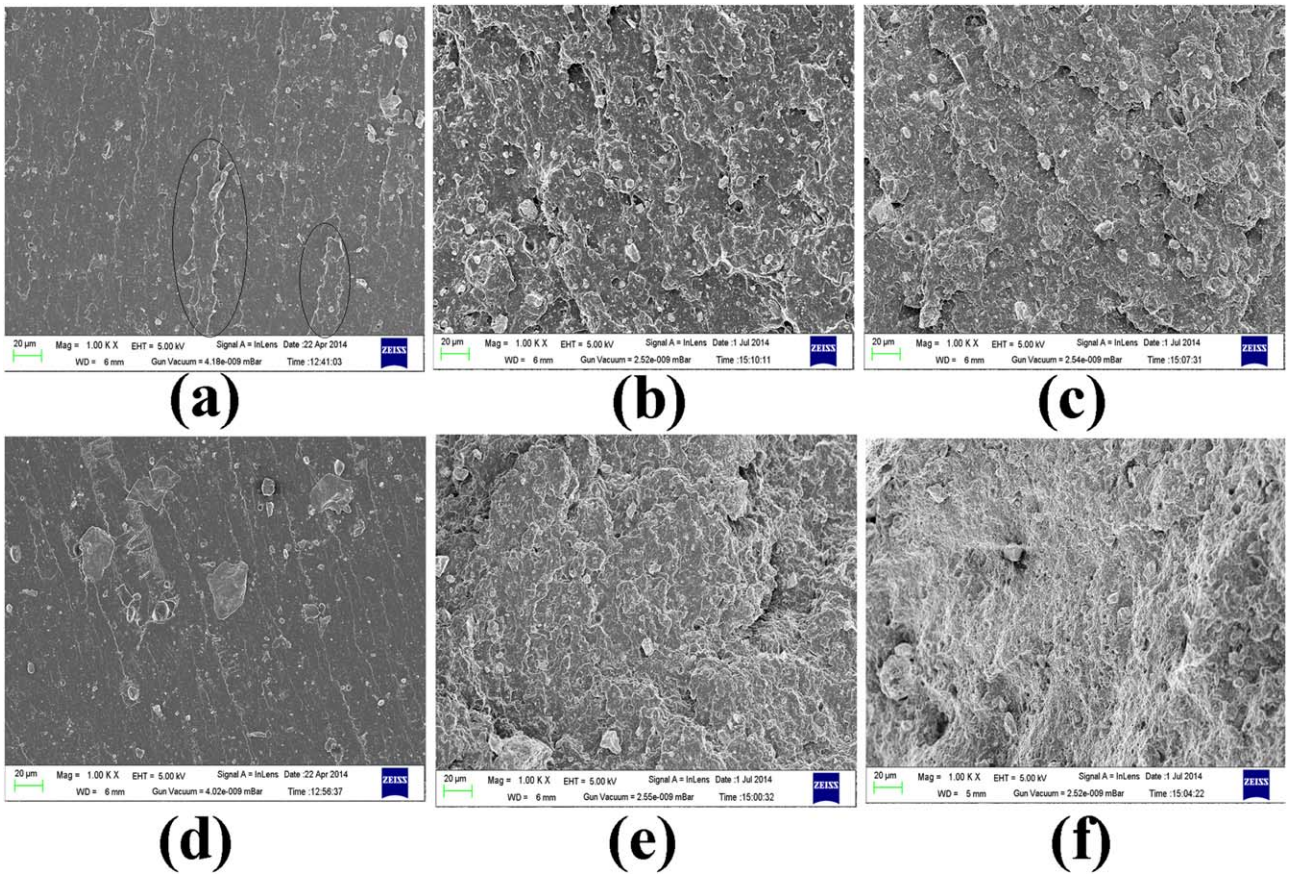

Figure 10. Tensile fracture surface of (a) NR-S-0 (b) NR-S-40 (c) NR-S-60 (d) CGNR-S-0 and (e) CGNR-S-40 (f) CGNR-S-60 at ×1000 magnification. [Color figure can be viewed in the online issue, which is available at wileyonlinelibrary.com.]

network, resulting in less or no recovery. Moreover, the compression set is lower for CGNR vulcanizates in comparison with that of NR vulcanizates at equivalent loadings of silica filler. It is observed that the compression set of CGNR vulcanizates at 40 phr loading of silica is found to be 26.7%, while that with NR vulcanizate is 31.0%. This may be explained on the basis of greater chain slippage during compressive loading and higher recovery on removal of stress. This has led to higher elastic recovery in the CGNR vulcanizates.

Fracture Analysis of the NR Vulcanizates before and after Grafting with Cardanol by Field Emission Scanning Electron Microscopy

Tensile Fracture Surface. The surface topology of the NR and CGNR vulcanizates with and without silica fillers after tensile fracture are shown in Figure 10(a–f), respectively. Figure 10(a,d) represent the fracture surface of the gum NR and CGNR vulcanizates respectively after tensile fracture whereas, Figure 10(b,e) represent the fracture surface of 40 phr silica filled NR and CGNR vulcanizates respectively. Figure 10(c,f) represent the fracture surface of 60 phr silica filled NR and CGNR vulcanizates, respectively.

Figure 10(a) shows the tensile fracture surface of the NR gum vulcanizate depicting a smooth and clear surface with flow lines, while under higher magnification [Figure 11(a)] crystallite structures are seen scattered on the surface, with convoluted flow lines indicating the dissipation of energy along the edges typical to the ductile type of failure. The tensile fracture surface of CGNR gum vulcanizate [Figure 10(d)] also exhibits a smooth and clear surface, but with very distinct and larger flow lines at 45° angle to the plane indicating enhanced ductile fracture. The fracture path is clearly visible in the magnified image [Figure 11(d)] which is obstructed by the presence of scattered crystal structures intermittently. The failure is totally ductile in nature.

The tensile fracture surface of 40 phr silica-filled NR vulcanizate [Figure 10(b)] shows a creepy type of failure surface with not so distinct flow lines. The presence of occasional vacuoles and particle clumps resulting from the dewetted silica is clearly visible which becomes more prominent under higher magnification [Figure 11(b)]. Figure 10(e) shows the tensile fracture surface of the 40 phr filled CGNR vulcanizates with no clear cut flow lines implying no systematic fracture path, but the creepy type of failure is still maintained as that observed for the NR vulcanizates at the same filler loading. The creepy type of fracture surface indicates a better compatibility between the filler and the rubber, resulting in ductile type of failure.[43,44] Moreover, it shows finer silica dispersion with fewer numbers of undispersed and dewetted silica on the surface, forming rosette type structures as observed under higher magnification [Figure 11(e)]. The higher dispersion of silica filler may be due to the additional interaction occurring between the cardanol phenolic

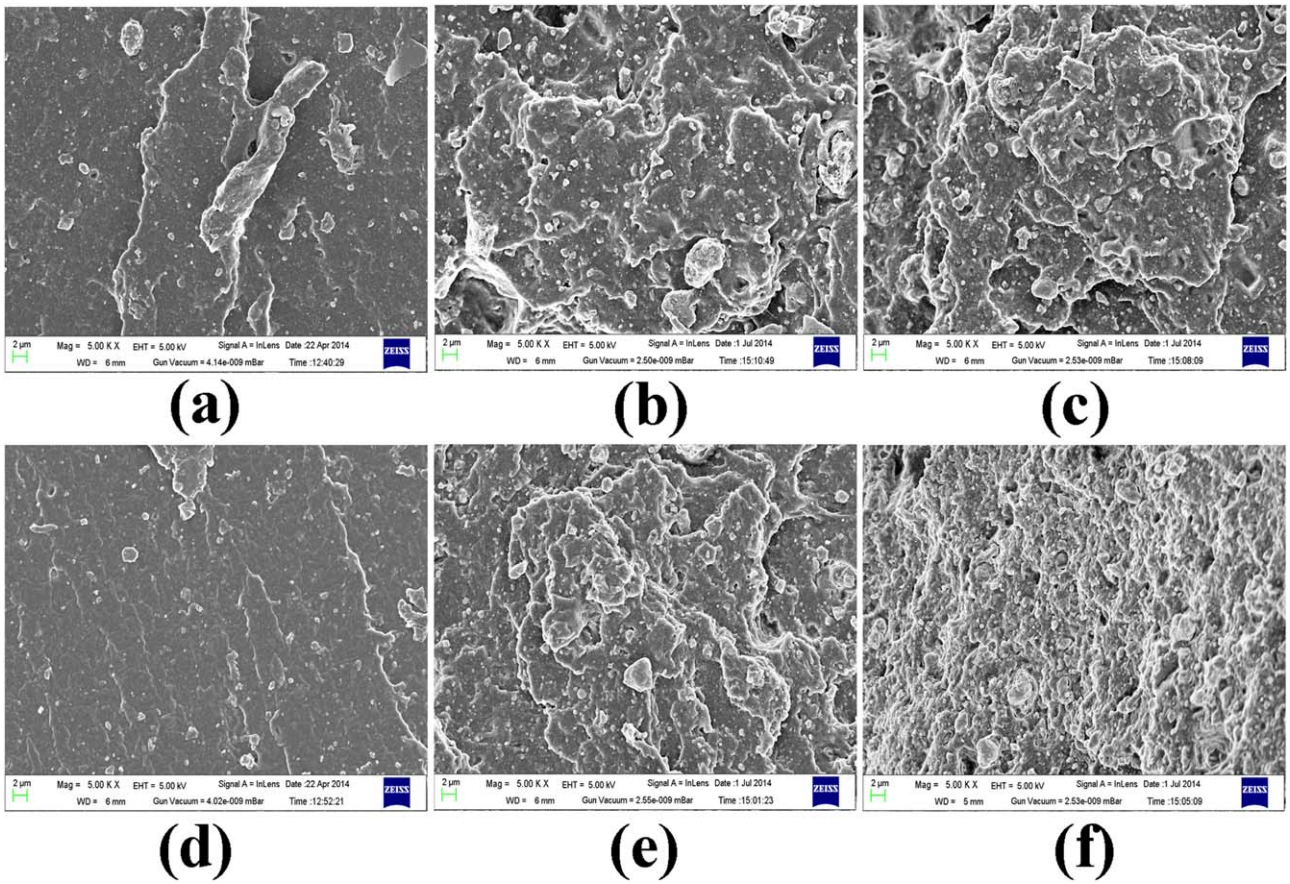

Figure 11. Tensile fracture surface of (a) NR-S-0 (b) NR-S-40 (c) NR-S-60 (d) CGNR-S-0 and (e) CGNR-S-40 (f) CGNR-S-60 at ×5000 magnification. [Color figure can be viewed in the online issue, which is available at wileyonlinelibrary.com.]

—OH groups and the silanol groups on the silica surface forming hydrogen bonds as discussed earlier and this is in consonance with the higher tensile strength observed for the 40 phr silica-filled CGNR vulcanizates (19.8 MPa) than that of the NR vulcanizate (17.5 MPa).

At higher filler concentration such as 60 phr silica loading, the tensile fracture surface of NR vulcanizates [Figure 10(c)] shows a creepy type of failure with higher numbers of silica agglomerates showing irregular flow lines and disgruntled scaly surface due to micro tear which can be seen more clearly under higher magnification [Figure 11(c)]. Figure 10(f) represents the tensile fracture surface of CGNR vulcanizates with 60 phr silica filler and it shows a fibrous matrix because of disgruntled flow paths making a tissue like appearance, with occasional smaller agglomeration. Under higher magnification [Figure 11(f)] it is seen to have fewer clumps of silica particles than that of the NR vulcanizates at equivalent filler loading, but with higher numbers of the dewetted silica particles than that of the 40 phr silica filled CGNR vulcanizates. This may be the reason for lowering of tensile strength at higher silica loadings in the rubber matrix because of the dilution effect and it exactly correlates with the tensile properties as depicted in Figure 9(a).

Abraded Surface. Abrasion of the rubber is a complex phenomenon and several researchers earlier have attempted to explain the mechanism of abrasion of rubber. During abrasion, detachment of small rubber particles of 1–5 μm size takes place, leaving behind pits on the surface. On continuous rubbing against sharper edges of the road surfaces, larger particles of the rubber, of the order of 0.1 mm are removed and a major weight loss is attributed to the loss of these larger particles.[45] Fukahori and Yamazaki[46] explained that the formation of the periodic surface patterns during rubber abrasion is contributed by two types of periodic motions; (i) initiation of cracks by microvibration with the natural frequency of the rubber and (ii) propagation of cracks by the stick-slip oscillation. They have explained that these two driving forces produce bimodal size distribution of abraded particles, small particles of the order of ten micrometres by microvibrations and large ones of the order of a few hundred micrometres by the stick-slip phenomenon.

Gent *et al.*[47] reported that abrasion of elastomers occur by two competitive mechanisms; (i) removal of microscopic particles of rubber by a fracture process and (ii) chemical deterioration of rubber at the surface region, initiated by the mechanical stress and promoted by oxygen in the atmosphere. Bhowmick *et al.*[48] have explained the abrasion phenomena by two mechanisms: (i) abrasive, which results from micro cutting by solid projections on the surface of the abrader body and (ii) frictional, which results from the forces of friction created by projections which deform the surface layers of the elastic material many times and

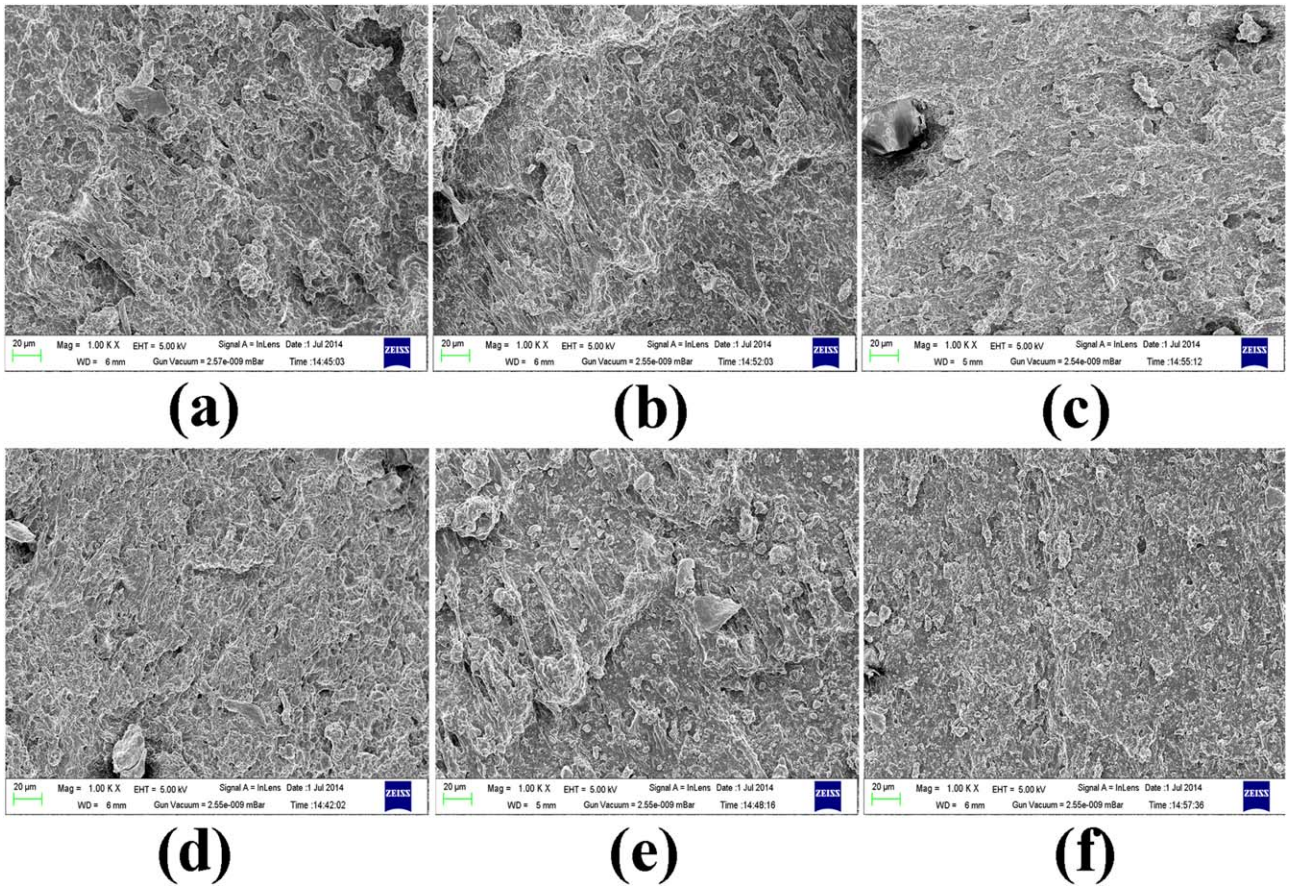

Figure 12. Abraded fracture surface at magnification of ×1000: (a) NR-S-0 (b) NR-S-40 (c) NR-S-60 (d) CGNR-S-0 and (e) CGNR-S-40 (f) CGNR-S-60. [Color figure can be viewed in the online issue, which is available at wileyonlinelibrary.com.]

separate them off without tearing. In the first type, longitudinal furrows are formed on the abraded surface and transverse ridges are formed in the second. They have established that the abrasive mechanism is followed by the gum vulcanizate while, the filled vulcanizates follow the frictional mechanism.

The FESEM photomicrographs of the abraded surface are presented in Figure 12(a–c) for NR vulcanizates and in Figure 12(d–f) for CGNR vulcanizates at filler loadings varying from zero (gum vulcanizate) to 40 and 60 phr, respectively at a magnification of 1000×. The abraded surface of the NR gum vulcanizate [Figure 12(a)] shows no definite patterns with a rough and disgruntled surface with small particle debris. However, at higher magnifications shown in Figure 13(a), the debrided surface is clearly visible, but the debris are not fully separated. The surface topography is closely similar to that of fatigue failure. This supports the higher abrasion loss as observed in Figure 9(e) corresponding to a value of 3.72 cm^3 hr^{-1}.

Similarly, abraded surface of CGNR gum vulcanizate [Figure 12(d)] shows no regular patterns, however in the magnified image [Figure 13(d)], initiation of ridges are clearly visible, without any visible debris, which accounts for its relatively lower abrasion loss (3.12 cm^3 hr^{-1}) as compared to that of gum NR vulcanizate. The surface topography is similar to fatigue type of failure. The lowering in abrasion loss may be explained as due to presence of grafted cardanol in CGNR which may cause slippage of the rubber and thus, reducing the frictional force between the abrader and the rubber surface during abrasion. Gent *et al.*[47] have reported that the presence of the oily products increase the resistance to abrasion, even when the frictional force maintained constant. It is assumed to form a viscous protective film; thus, alleviating the local concentrations of tearing force that are presumably responsible for the detachment of wear particles.

Incorporation of silica filler in to the rubber matrix increases the abrasion resistance tremendously. This may be observed from the Figure 12(b,c) for NR vulcanizates and Figure 12(e,f) for CGNR vulcanizates. Figure 12(b) shows the abraded surface of NR vulcanizate containing 40 phr silica filler and it can be seen that there are prominent ridges formed with small amount of dewetted silica containing debris on the surface and at a higher magnification of 5000× [Figure 13(b)], deep furrows are observed and the matrix is highly strained. The abraded surface of NR vulcanizate with 60 phr silica loading [Figure 12(c)] at magnification of 1000× shows a coarse and rumpled surface, while under higher magnification [Figure 13(c)] finer ridges with dimples are observed.

The FESEM photomicrographs of CGNR vulcanizates with 40 phr silica loading [Figure 12(e)] shows a coarse-ribbed structure

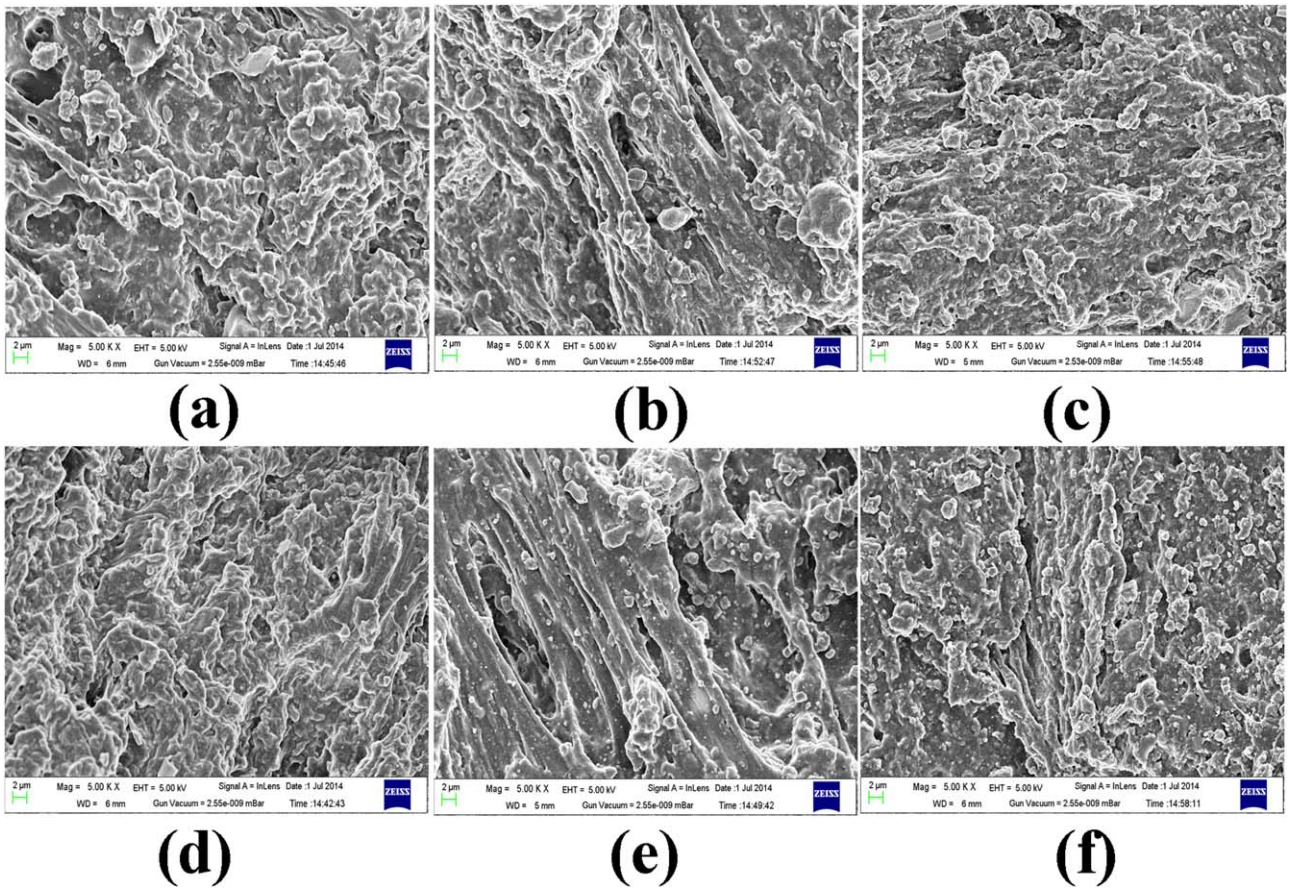

Figure 13. Abraded fracture surface at magnification of ×5000: (a) NR-S-0 (b) NR-S-40 (c) NR-S-60 (d) CGNR-S-0 and (e) CGNR-S-40 (f) CGNR-S-60. [Color figure can be viewed in the online issue, which is available at wileyonlinelibrary.com.]

with narrower spacings in comparison with that of NR vulcanizate at equivalent loadings and the magnified image at 5000× [Figure 13(e)] shows rather rough and cellular structure with finer ridges. Finer ridges with narrower spacings on the abraded surface indicative of higher abrasion resistance.[49] The finer ridges with narrower spacings as observed in the 40 phr silica filled CGNR vulcanizates accounts for its lower abrasion loss (2.10 cm^3 hr^{-1}) in comparison with its NR counterpart (2.84 cm^3 hr^{-1}). The abraded surface of CGNR vulcanizates at 60 phr of silica loading shows a coarse surface as shown in Figure 12(f). A higher magnification of the abraded surface [Figure 13(f)] shows clearly a fine coral tree or roughly bony structures. This may account for the lowest abrasion loss (1.12 cm^3 hr^{-1}) observed for the CGNR vulcanizates at 60 phr silica loadings. It is observed that at all loadings of the filler, the CGNR vulcanizates show better ridge formation in comparison with that of the NR vulcanizates at equivalent filler loading. This explains the reduction in abrasion loss in case of CGNR vulcanizates as compared to that of the NR vulcanizates as shown in Figure 9(e).

Dispersion Study by High Resolution Transmission Electron Microscopy (HRTEM)

Figure 14(a–d) shows the HRTEM images of the NR and CGNR vulcanizates, filled with 40 and 60 phr of precipitated silica. Figure 14(a) shows the dispersion of silica in NR containing 40 of the filler. It shows the dispersion of silica is uniform throughout the rubber matrix with few agglomerated structures scattered here and there. Figure 14(c) shows the dispersion of silica in CGNR matrix at 40 phr of the silica filler. Here, the silica particles are well dispersed in the rubbery matrix and the dispersion seems to be much uniform and finer. The filler particles are distributed uniformly with less agglomeration than that observed for the NR vulcanizates at the same filler loading. Thus, it may be inferred that cardanol grafted natural rubber has better dispersion of the silica filler in the matrix as compared to that of the unmodified NR. This may be because of the additional rubber–filler interaction between the phenolic moiety of cardanol and surface functional groups on the silica particles which may take place within the cardanol grafted natural rubber matrix, thus enhancing the dispersion of the filler particles in the CGNR matrix. This is considered to be the reason of better reinforcement imparted by the silica filler in CGNR matrix resulting in superior physico-mechanical properties in comparison with that of NR vulcanizates owing to the uniform and homogenous dispersion of the silica particles in the rubber matrix. Figure 14(b,d), respectively shows the dispersion at higher loading of 60 phr of silica filler in the NR and CGNR vulcanizates. The dispersion of the silica filler in both the matrices appear to be almost similar except that the number

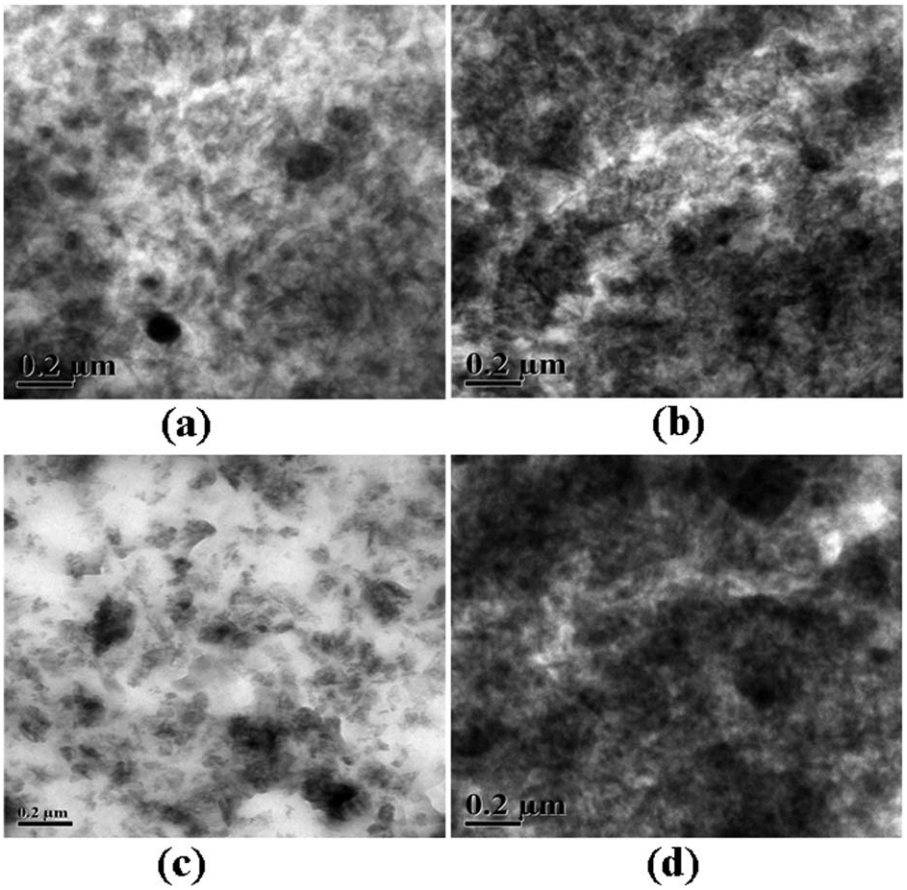

Figure 14. HRTEM photomicrographs of (a) NR-S-40, (b) NR-S-60, (c) CGNR-S-40 and (d) CGNR-S-60.

of agglomerated silica structures seems to be higher than that observed for the 40 phr silica filler loaded rubber matrices. This may be the reason for lower tensile strength of the matrices at 60 phr silica filler loadings than that observed for the 40 phr silica-filled rubber vulcanizates.

Dynamic Mechanical Analysis of the Silica Filled NR and CGNR Vulcanizates

The dependency of dynamic storage modulus, E' and damping factor, tan δ on the temperature are presented in Figure 15(a,b), respectively in the temperature range varying from -80°C to $+100$°C for the NR and CGNR vulcanizates filled with silica filler. From Figure 15(a) it is observed that with an increase in silica loadings, the dynamic storage modulus (E') increases in case of both the NR and CGNR vulcanizates throughout the temperature range studied, particularly below the glass transition temperature. This has been attributed to an increase in stiffening offered by the adsorption of polymer molecular chains on the filler surface as reported by Wang *et al.*[5] This adsorption reduces the mobility of the polymer segments and results in a rubber shell on the filler surface. The reduced mobility and the formation of the rubber shell increases the polymer viscosity which ultimately increases the storage modulus.

The storage modulus for the gum CGNR is found to be higher than that of the gum NR vulcanizate particularly below the glass transition temperature region. This may be explained on the basis of higher hydrodynamic volume of the CGNR as a result of grafting of cardanol on to NR backbone. However, for the filled vulcanizates, the storage moduli for the filled CGNR vulcanizates are found to be comparable to that corresponding to NR vulcanizate at similar loading of silica. The results obtained from the dynamic mechanical analyses are in good agreement with the physico-mechanical properties of the silica-filled NR and CGNR vulcanizates. It can be seen that the tensile moduli of both the rubber matrices are comparable at each loadings of the silica filler as shown in Figure 9(b).

The relationship between the loss factor (tan δ) and temperature for the gum as well as silica filled NR and CGNR vulcanizates is presented in Figure 15(b). It is observed that the maximum loss tangent (tan δ_{max}) is marginally shifted toward a lower temperature for the CGNR vulcanizates at all loadings of silica in comparison with that of natural rubber confirming the plasticization effect of cardanol when grafted on to the NR. The glass transition temperature (T_g) of the gum CGNR vulcanizate is found to be -51.8°C, while that for the gum NR vulcanizate it is -48.4°C which confirms the inherent plasticizing effect of the grafted cardanol. In general, plasticizers cause lowering of T_g by configuring between the polymer chains. This alters the polymer-polymer interactions and enhances chain mobility. The α- relaxation peak height (tan δ_{max}) is observed to be lowered with increase in silica content for both the NR and CGNR vulcanizates. The intensity of the tan δ peak at the glass transition

temperature reflects the extent of mobility of the macromolecular chain segments in that region. Any restriction in the main chain mobility of the polymer is expected to decrease the area under the loss modulus curve versus temperature and this trend has been reflected in the intensity of the tan δ peak.[50] The tan δ peak for the CGNR vulcanizates is found to be lower than that of the NR vulcanizates.

The loss tangent of NR and CGNR vulcanizates at 0°C and +60°C is reported in Table IV. The tan δ at 0°C reflects the wet grip property; thus, the higher the value of tan δ at 0°C leads to a better wet grip property. However, from Table IV, it can be seen that the value of tan δ at 0°C is lower for the CGNR vulcanizates in comparison to that of NR vulcanizates which means poorer wet grip characteristics for the CGNR vulcanizates. The tan δ at around 60°C reflects the rolling resistance property of the tires. The smaller the value of tan δ at 60°C, the lower the rolling resistance and better is the fuel economy.[51] From Table IV, it can be seen that the value of tan δ at 60°C is found to be lower for the cardanol grafted natural rubber in comparison with that of the natural rubber at all loadings of silica filler, which imply a better rolling resistance for the CGNR vulcanizates. This may be explained on the basis of improved filler dispersion and lower frictional forces acting on the surface of the cardanol grafted natural rubber.

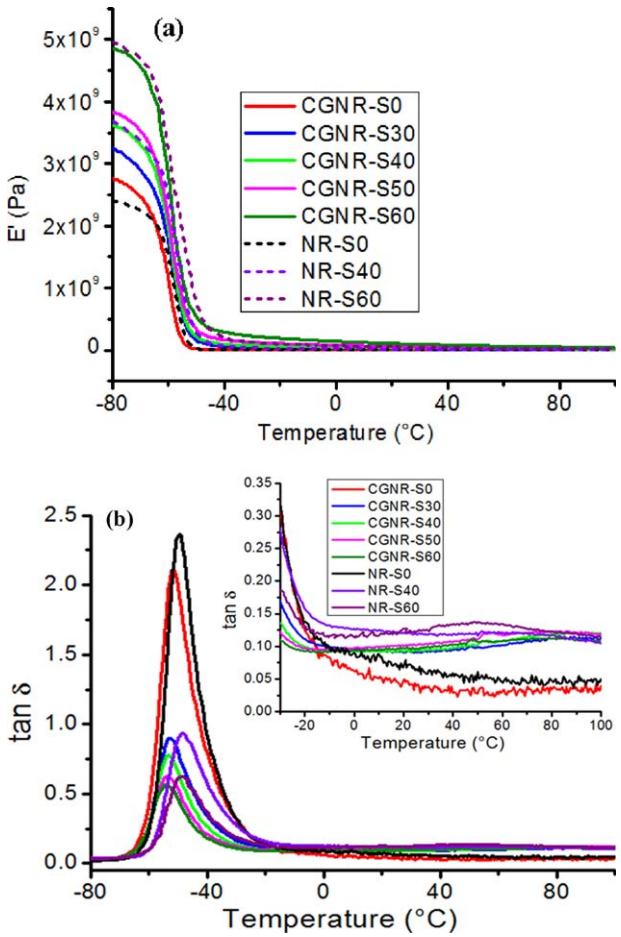

Figure 15. Effect of (a) dynamic storage modulus (E') and (b) loss factor (tan δ) as a function of temperature for silica filled NR and CGNR vulcanizates. [Color figure can be viewed in the online issue, which is available at wileyonlinelibrary.com.]

Table IV. Loss Tangent (Tan δ) Values for the NR and CGNR Vulcanizates

	CGNR			NR		
Tan δ at	C-0	C-40	C-60	C-0	C-40	C-60
0°C	0.063	0.093	0.094	0.087	0.126	0.114
60°C	0.031	0.108	0.110	0.048	0.121	0.134

CONCLUSION

The physico-mechanical properties of the CGNR vulcanizates are found to be better than that of the natural rubber vulcanizates. Moreover, cardanol after grafting acts as a cure-activator at all loadings of silica varying from 30 to 60 phr, because of the additional unsaturation present in the aliphatic side chain of cardanol moiety which takes part in the vulcanization reaction efficiently. The crosslink density and the bound rubber content are found to be higher for the cardanol grafted natural rubber as compared to NR as a result of hydrogen bond formation between the phenolic hydroxyl group of the cardanol present in the CGNR matrix and the surface functional groups present on the silica fillers. This accounts for a better polymer-filler interaction in case of the CGNR matrix which has been confirmed by the Cunnen–Russel plot, Kraus plot and also from the lower Payne effect as observed for the silica filled CGNR vulcanizates in comparison with that of NR vulcanizates at the same filler loadings. The tensile strength, tear strength, abrasion resistance, and compression set are found to be better for the CGNR vulcanizates. The fracture analysis through FESEM study supports the findings for the higher tensile properties and lower abrasion loss of the CGNR vulcanizates in comparison with that of NR vulcanizates at similar silica loadings. The dispersion study through HRTEM exhibit better dispersion of silica filler in CGNR matrix as compared to that observed for NR matrix. The CGNR vulcanizates show lower rolling resistance in comparison with that of NR vulcanizates filled with silica at equivalent loadings. In conclusion, cardanol acts as a dispersion enhancer in the rubber matrix imparting better rubber–filler interaction and thus, leading to higher reinforcement. In future, it may emerge as a new commercial grade of natural rubber, with technical and economic advantages.

ACKNOWLEDGMENTS

One of the authors Miss Sunita Mohapatra is grateful to the Council of Scientific and Industrial Research (CSIR), New Delhi, India for the award of individual Senior Research Fellowship for carrying out this work. The authors thank the Director, Rubber Board, Kottayam, India for supplying natural rubber latex and providing facility for large scale grafting of cardanol on to natural rubber.

REFERENCES

1. Rubber Statistical Bulletin (**2014**) January-March. Available at: http://www.rubberstudy.com/documents/WebSiteData_3.0c.pdf. Accessed 3rd May **2014**.
2. The Trend. *Rubber Stat. News* **2014**, *72*, 1. Available at: http://clinic.rubberboard.org.in/PDF/RSNews032014.pdf. Accessed 3rd May, **2014**.
3. Sittiphan, T.; Prasassarakich, P.; Poompradub, S. *Mater. Sci. Eng. B Adv.* **2014**, *181*, 39.
4. Kaewsakul, W.; Sahakaro, K.; Dierkes, W. K.; Noordermeer, J. W. M. *Rubber Chem. Technol.* **2012**, *85*, 277.
5. Wang, M. J. *Rubber Chem. Technol.* **1998**, *71*, 520.
6. Lin, Y.; Zhang, A.; Sun, J.; Wang, L. *J. Macromol. Sci. B Phys.* **2013**, *52*, 1494.
7. Sae-Oui, P.; Rakdee, C.; Thanmathorn, P. *J. Appl. Polym. Sci.* **2002**, *83*, 2485.
8. Sarkawi, S. S.; Dierkes, W. K.; Noordermeer, J. W. M. *Rubber Chem. Technol.* **2014**, *87*, 103.
9. Meon, W.; Blume, A.; Luginsland, H.-D.; Uhrlandt, S. In Rubber Compounding: Chemistry and Applications; Rodgers, B., Ed.; Marcel Dekker, Inc.: New York, **2004**; Chapter 7.
10. Mohapatra, S.; Nando, G. B. *RSC Adv.* **2014**, *4*, 15406.
11. Maia, F. J. N.; Ribeiro, F. W. P.; Rangel, J. H. G.; Lomonaco, D.; Luna, F. M. T.; Lima-Neto, P. D.; Correia, A. N.; Mazzetto, S. E. *Indus. Crops Prod.* **2015**, *67*, 281.
12. Telascrêa, M.; Leão, A. L.; Ferreira, M. Z.; Pupo, H. F. F.; Cherian, B. M.; Narine, S. *Mol. Cryst. Liq. Cryst.* **2014**, *604*, 222.
13. Yadav, R.; Devi, A.; Tripathi, G.; Srivastava, D. *Eur. Polym. J.* **2007**, *43*, 3531.
14. Vu, Y. T.; Mark, J. E.; Pham, L. H. *Polym. Plast. Technol. Eng.* **1999**, *38*, 189.
15. Antony, R.; Pillai, C. K. S. *J. Appl. Polym. Sci.* **1994**, *54*, 429.
16. Manjula, S.; Pillai, C. K. S.; Kumar, V. G. *Thermochim. Acta* **1990**, *159*, 255.
17. Sharma, P.; Shukla, S.; Lochab, B.; Kumar, D.; Kumar Roy, P. *Mater. Lett.* **2014**, *133*, 266.
18. Kathalewar, M.; Sabnis, A. *J. Coat. Technol. Res.* **2014**, *11*, 601.
19. Gong, Z. L.; Cen, L.; Wang, S. T.; Chen, F. L. *J. Appl. Polym. Sci.* **2014**, *131*, 40462(1–7), doi:10.1002/app.40462.
20. Rodrigues, F. H. A.; Feitosa, J. P. A.; Ricardo, N. M. P. S.; França, F. C. F.; Carioca, J. O. B. *J. Braz. Chem. Soc.* **2006**, *17*, 265.
21. Menon, A. R. R.; Pillai, C. K. S.; Jin, W. S.; Nah, C. *Polym. Int.* **2005**, *54*, 629.
22. Menon, A. R. R.; Pillai, C. K. S.; Nando, G. B. *Polymer* **1998**, *39*, 4033.
23. Menon, A. R. R. *J. Fire Sci.* **1997**, *15*, 3.
24. Menon, A. R. R.; Pillai, C. K. S.; Nando, G. B. *J. Adhes. Sci. Technol.* **1995**, *9*, 443.
25. Wolff, S.; Wang, M.-J. In Carbon Black: Science and Technology; Donnet, J.-B., Bansal, R. C., Wang, M.-J., Eds.; Marcel Dekker Inc.: New York, **1993**; Chapter 9.
26. Boonstra, B. B. S. T.; Dannenberg, E. M. *Rubber Chem. Technol.* **1959**, *32*, 825.
27. Sombatsompop, N.; Kumnuantip, C. *J. Appl. Polym. Sci.* **2003**, *87*, 1723.
28. Ellis, B.; Welding, G. N. R. *Chem. Technol.* **1964**, *37*, 571.
29. Ansarifar, A.; Nijhawan, R.; Nanapoolsin, T.; Song, M. *Rubber Chem. Technol.* **2003**, *76*, 1290.
30. Menon, A. R. R.; Pillai, C. K. S.; Nando, G. B. *J. Appl. Polym. Sci.* **1994**, *51*, 2157.
31. Mohapatra, S.; Nando, G. B. *Rubber Chem. Technol.* **2015**, *88*, 289.
32. Morrison, N. J.; Porter, M. *Rubber Chem. Technol.* **1984**, *57*, 63.
33. Krejsa, M. R.; Koenig, J. L. *Rubber Chem. Technol.* **1993**, *66*, 376.
34. Choi, S. S.; Nah, C.; Jo, B. W. *Polym. Int.* **2003**, *52*, 1382.
35. Roychoudhury, A.; De, P. P. *J. Appl. Polym. Sci.* **1995**, *55*, 9.
36. Rooj, S.; Das, A.; Stockelhuber, K. W.; Wang, D. Y.; Galiatsatos, V.; Heinrich, G. *Soft Matter* **2013**, *9*, 3798.
37. Kraus, G. *J. Appl. Polym. Sci.* **1963**, *7*, 861.
38. Luo, Y. Y.; Wang, Y. Q.; Zhong, J. P.; He, C. Z.; Li, Y. Z.; Peng, Z. *J. Inorg. Organometallic Polym. Mater.* **2011**, *21*, 777.
39. Ma, J. H.; Zhang, L. Q.; Wu, Y. P. *J. Macromol. Sci. B: Phys.* **2013**, *52*, 1128.
40. Zhao, F.; Shi, X.; Chen, X.; Zhao, S. *J. Appl. Polym. Sci.* **2010**, *117*, 1168.
41. Fröhlich, J.; Niedermeier, W.; Luginsland, H. D. *Compos. A Appl. Sci. Manufact.* **2005**, *36*, 449.
42. Mostafa, A.; Abouel-Kasem, A.; Bayoumi, M. R.; El-Sebaie, M. G. *Mater. Des.* **2009**, *30*, 1561.
43. Idrus, S. S.; Ismail, H.; Palaniandy, S. *Polym. Plast. Technol. Eng.* **2011**, *50*, 1.
44. Pal, P. K.; De, S. K. *Rubber Chem. Technol.* **1982**, *55*, 1370.
45. Muhr, A. H.; Roberts, A. D. *Wear* **1992**, *158*, 213.
46. Fukahori, Y.; Yamazaki, H. *Wear* **1994**, *171*, 195.
47. Gent, A. N.; Pulford, C. T. R. *J. Appl. Polym. Sci.* **1983**, *28*, 943.
48. Bhowmick, A. K.; Nando, G. B.; Basu, S.; De, S. K. *Rubber Chem. Technol.* **1980**, *53*, 327.
49. Tabsan, N.; Wirasate, S.; Suchiva, K. *Wear* **2010**, *269*, 394.
50. Perera, M. C. S. *J. Polym. Sci. B: Polym. Phys.* **1999**, *37*, 1141.
51. Seo, B.; Kim, H.; Paik, H.; Kwag, G.; Kim, W. *Macromol. Res.* **2013**, *21*, 738.